

## Variable-temperature and variable-pressure studies of small-molecule organic crystals

Elena V. Boldyreva,<sup>\*1,2</sup> Tatyana N. Drebushchak,<sup>1,2</sup> Tatyana P. Shakhtshneider,<sup>1,2</sup> Heidrun Sowa,<sup>3</sup> Hans Ahsbals,<sup>3</sup> Sergei V. Goryainov,<sup>1,4</sup> Svetlana N. Ivashevskaya,<sup>1,5</sup> Evgeniya N. Kolesnik,<sup>1,2</sup> Valeri A. Drebushchak,<sup>1,4</sup> and Elena B. Burgina<sup>1,6</sup>

<sup>1</sup> REC-008 "Molecular Design and Ecologically Safe Technologies", Novosibirsk State University, Pirogova 2, Novosibirsk 630090 Russia,

<sup>2</sup> Institute of Solid State Chemistry SB RAS, Novosibirsk, Russia;

<sup>3</sup> Philipps-Universitaet Marburg, Hans-Meerwein Strasse, D-35032 Marburg/Lahn, Germany

<sup>4</sup> Institute of Mineralogy and Petrography SB RAS, Novosibirsk, Russia;

<sup>5</sup> Institute of Geology Karelian Scientific Center RAS, Petrozavodsk, Russia;

<sup>6</sup> Borekov Institute of Catalysis SB RAS, Novosibirsk, Russia

E-mail: [boldyrev@nsu.ru](mailto:boldyrev@nsu.ru)

Dedicated to Professor Alexander I. Konovalov on the occasion of his 70<sup>th</sup> anniversary

(received 11 Nov 04; accepted 21 Feb 05; published on the web 02 Mar 05)

---

### Abstract

Several examples of the comparative variable-temperature and variable-pressure studies of the small-molecule organic crystals are discussed. Selected systems represent the crystals with non-spherical flexible molecules / molecular fragments and with different types of intermolecular interactions, ranging from van der Waals interactions to hydrogen bonds of various types (OH...O, NH...OH, NH...O=C). A special attention is paid to the studies of solid drugs (polymorphs of paracetamol), amino acids (polymorphs of glycine, L-serine, D,L-serine), and dipeptides (glycylglycine and glycylglycine hydrate) by structural, spectroscopic and calorimetric techniques. The anisotropy of structural distortion within the range of stability of the same phase, as well as the phase transitions induced by changes in temperature or pressure are discussed.

**Keywords:** Hydrogen bonds, high pressure, amino acids, polymorphs, phase transitions

---

### Introduction

The majority of crystal structures of organic molecules have been determined at normal pressure conditions. Low temperatures are used rather often for structure determination, in order to suppress molecular motions and thus to improve the data quality. At the same time, there is a

great demand for the observations of structural *changes* that occur in organic solids in response to *variations* in pressure or in temperature.<sup>1-14</sup> Apart from many other interesting aspects of variable-temperature and variable-pressure organic crystal studies, including correlations “structure-properties” for new materials and devices, such observations are necessary to assess the theoretical interaction models used to predict crystal packings and conformations of molecules by the minimization of total non-bonded potential energy, to gain control over polymorphism of these compounds, to find the factors determining their relative thermodynamic and kinetic stability.

A molecular crystal is a “supramolecular entity par excellence”. It is formed as a result of self-recognition and self-assembling, and its structure results from a complex interplay of multiple weak non-covalent intermolecular interactions, such as hydrogen bonds of various types, van der Waals interactions,  $\pi$   $\pi$  interactions, etc. The crystal structure is very sensitive to such parameters as temperature and pressure, and the structural response to variations in temperature / pressure (anisotropic continuous changes in cell parameters and volume, or a phase transition) can be used as a tool of probing the interactions in the crystal.

In the present paper this will be illustrated at several examples of recent studies by the authors of this paper, such as a study of the polymorphs of paracetamol, a study of the polymorphs of glycine, the studies of L- and D, L-serine, of glycylglycine and glycylglycine hydrate. More examples of very careful diffraction, spectroscopic, calorimetry studies can be found in the review papers<sup>1-14</sup> and in the papers cited therein.

## Results and Discussion

### Polymorphs of paracetamol

Paracetamol (acetaminophen, panadol) (Figure 1) is an analgesic drug that is used worldwide in the manufacture of many millions of tablets and other dosage forms every year. Three polymorphs were reported for this compound,<sup>15-18</sup> but only for two of them it was possible to get single crystals thus enabling unambiguous structure solution. For the polymorph III a structural model was suggested on the basis of computing simulations,<sup>19</sup> and a comparison of these calculations with a powder diffraction pattern<sup>18</sup>. In the present contribution we shall restrict our discussion by two polymorphs only, for which the crystal structures were determined unambiguously from single-crystal X-ray diffraction experiments.<sup>15, 16</sup>

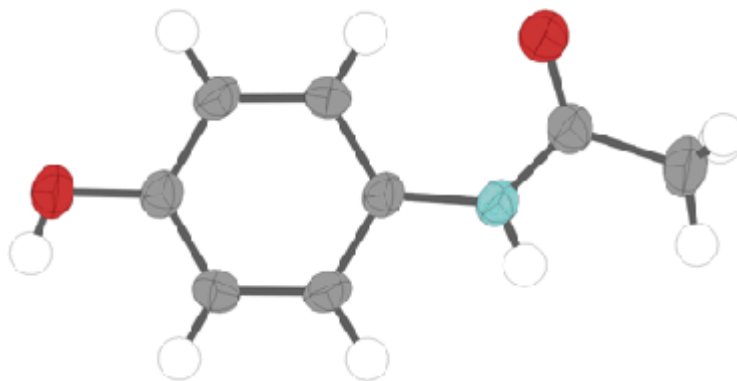


**Figure 1.** A molecule of paracetamol. Red – O, blue – N, grey – C, white – H.

Paracetamol I is monoclinic (space group symmetry  $P2_1/n$ ),<sup>16</sup> paracetamol II is orthorhombic (space group symmetry  $Pbca$ ).<sup>15</sup> In contrast to the stable polymorph I, the metastable polymorph II can be used for direct compression into tablets,<sup>20-22</sup> and was also reported to dissolve faster in water.<sup>21, 22</sup> The two polymorphs of paracetamol can be considered as examples of molecular crystals, in which topologically identical H-bonded chains of molecules are linked differently into two-dimensional layers,<sup>23</sup> and this results in the differences in the stability, various physical properties, dissolution behavior.

We have compared the thermodynamic functions of the two paracetamol polymorphs (using DSC and adiabatic calorimetry), as well as the structural response of the two polymorphs to variations in temperature and pressure (using powder and single-crystal X-ray diffraction and IR-spectroscopy).<sup>8,12,13,23-27</sup>

### Thermodynamic studies

A typical DSC-thermogram measured when heating a single crystal of paracetamol II is shown in Figure 2. Two endothermic events were observed. A small peak was observed at different temperatures  $T_{tr}$  for different crystals in a rather wide range (about 20 degrees) around 393°K. The shape of this peak was asymmetric and “inverted” as compared with the shape of a typical DSC-peak corresponding to melting. This can be an evidence of an “overheated transformation”. For several samples, heating was stopped immediately after this small endothermic peak was observed. After cooling a sample back to ambient temperature, no changes in the habit of the crystal were observed. The angles between the edges were sharp and there was no evidence that fusion could have taken place (Figure 3a). The crystal became opaque. X-ray diffraction showed that the sample was not a single crystal of the paracetamol II any longer, but a polycrystalline pseudomorph of paracetamol I (Figure 3b). Even a slight mechanical action at the pseudomorph was enough to destroy the pseudomorph – the shape of the starting single crystal of paracetamol II was preserved only because of the adhesion of small crystallites of paracetamol I. Thus, the endothermic event at about 393°K was proved to be an overheated single-crystal-to-polycrystal polymorphic transformation of paracetamol II into paracetamol I. Further heating resulted in the

melting of the monoclinic paracetamol I (the second, larger endothermic peak at 442°K, Figure 2). The enthalpy of II  $\rightarrow$  I polymorphic transition near 393°K ranged from 3.3 to 3.8 J/g (540 J/mol). For comparison, the enthalpy of melting of polymorph I is 50 times greater (176-182 J/g = 27 kJ/mol)<sup>27</sup>.

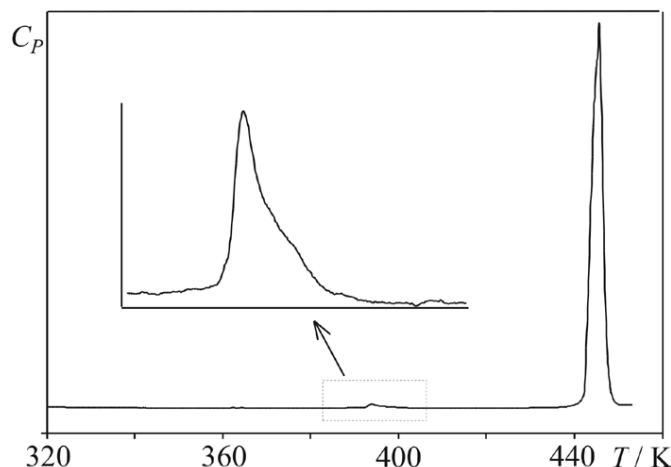


**Figure 2.** A DSC thermogram of paracetamol II above ambient temperature.<sup>27</sup>

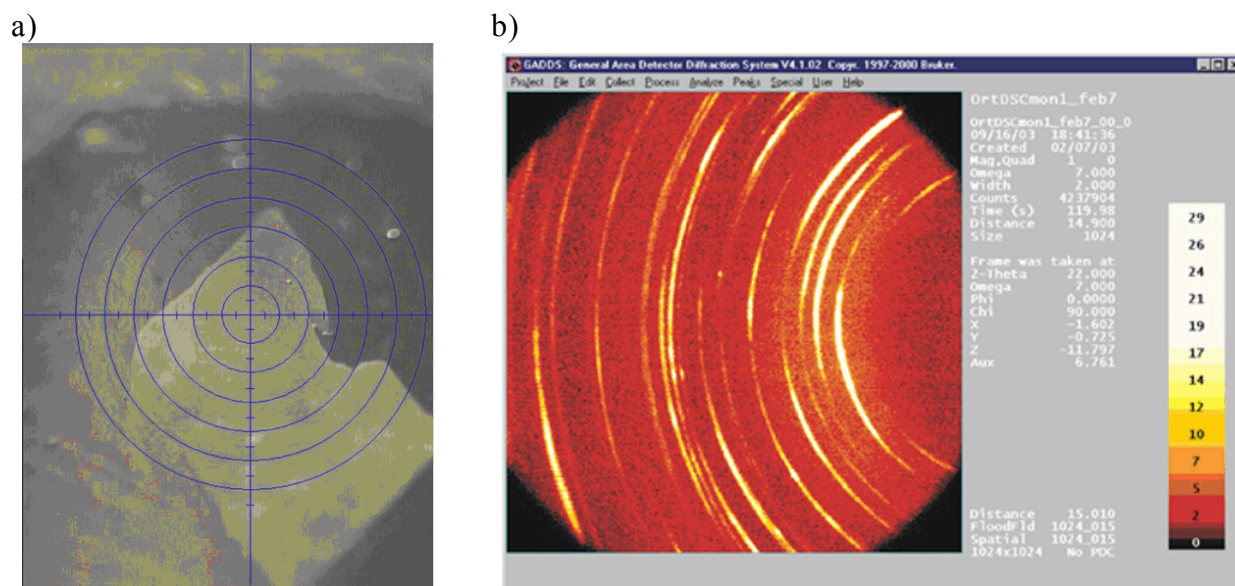


**Figure 3.** A paracetamol crystal (initially – orthorhombic) after its transformation into the monoclinic pseudomorph (a), and its powder diffraction pattern (b).<sup>27</sup>

A solid-state transformation of the individual crystals of paracetamol II into paracetamol I was observed also upon storage at ambient temperature, and was facilitated by the presence of water vapor. When a sample was measured by low-temperature calorimetry (temperature varied down to 5 K and then back to ambient), freezing and melting of water inclusions at about 273 K was accompanied by a polymorphic transformation of paracetamol II to paracetamol I.

The measurements of the heat capacity in a wide temperature range have allowed us to calculate the thermodynamic functions – enthalpy, entropy, free energy – for the two polymorphs of paracetamol.<sup>27</sup> The difference in the Gibbs energy  $\Delta G = G_{\text{orth}} - G_{\text{mon}}$  has two terms:  $[H_{\text{orth}}(T) - H_{\text{orth}}(0) - H_{\text{mon}}(T) + H_{\text{mon}}(0)] - T[S_{\text{orth}}(T) - S_{\text{mon}}(T)]$  and  $H_{\text{orth}}(0) - H_{\text{mon}}(0)$ . The first of them can be calculated based on the measurements of heat capacity. For the paracetamol polymorphs this value is positive in all the temperature range studied in the experiments (5 K – 300 K) and does not exceed 100 J/mol (Figure 4). This can be considered as an evidence of a slightly higher thermodynamic stability of the monoclinic polymorph as compared to the orthorhombic form, what is in a good agreement with the experimental observation of the orthorhombic-to-monoclinic transformation in a wide temperature range, also at low temperatures. The second term – the difference in the heats of formation – cannot be estimated without very delicate extra experiments, for example, comparing the heats of dissolution or sublimation of the two forms. From general consideration, it can reach several hundred J/mol, thus affecting noticeably the total value of  $\Delta G$ . The contribution to the heat capacity from the water solution inclusions (unavoidably present in the single crystals of the orthorhombic paracetamol)<sup>27,28</sup> The endothermic effect ( $\Delta H_{\text{tr}} = 540$  J/mol) measured for the non-equilibrium transformation from the less stable orthorhombic to the more stable monoclinic form<sup>27</sup> (which should be expected to be exothermic)<sup>29</sup> can be interpreted if one considers the endothermic contribution due to the evaporation of the water inclusions accompanying a polymorphic transformation and the resulting fragmentation of a crystal. The content of water in the crystals of the orthorhombic form could be estimated as 0.13 %.<sup>27,28</sup> The evaporation of this amount of water would contribute 2.9 J/g of paracetamol (440 J/mol of paracetamol) to the total heat of the polymorphic transformation of the orthorhombic form to the monoclinic one (the evaporation heat of water being 2260 J/g),<sup>30</sup> thus inverting the resulting sign of the value.

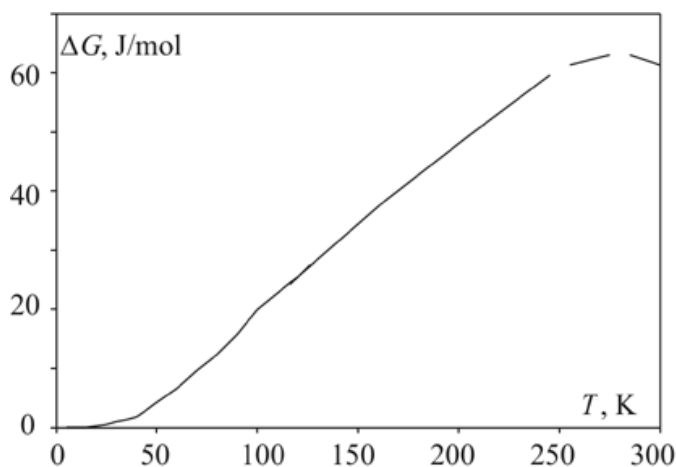


**Figure 4.** Difference in the Gibbs energy (orthorhombic – monoclinic, calorimetric part) versus temperature for the polymorphs I and II of paracetamol. At temperatures above 250 K the value is shown by the dashed line to stress a lower accuracy of the calculations in this range.

The monoclinic polymorph I was shown to be thermodynamically more stable than the orthorhombic form II in a wide temperature range, however, a transformation of the polymorph II into the polymorph I was obviously kinetically hindered, and could be facilitated by the presence of water. This fact is rather typical for the molecular organic crystals. The difference in the free energy between the polymorphs is much smaller than the barrier that must be overcome, in order to accomplish the structural reorganization.

Figure 5 shows the similarities and the differences in the molecular packing in the two polymorphs of paracetamol. Both structures are built from the chains, in which the paracetamol molecules are linked via OH...O hydrogen bonds. The chains are very similar in the two polymorphs. What is different, is the way how these chains are linked with each other via NH...O bonds, to give 2D-layers – flat (in the orthorhombic form), or corrugated (in the monoclinic polymorph). The hydrogen bonds OH...O within a chain are stronger than the NH...O hydrogen bonds between the chains. The chains can be considered as a “structure-forming synthones”,<sup>31</sup> and are preserved not only in the two polymorphs of paracetamol, but also in several adducts of paracetamol with other organic molecules<sup>32, 33</sup> (although they are only partly preserved in a methanol solvate,<sup>34</sup> and are no longer present in paracetamol hydrates).<sup>35,36</sup>

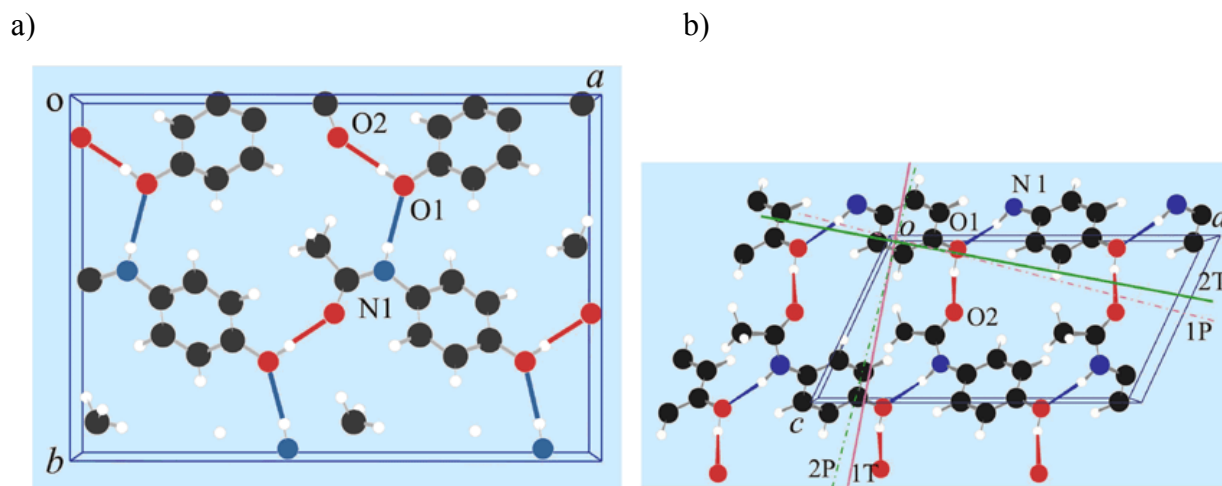


**Figure 5.** Fragments of crystal structures of the a) monoclinic (I), b) orthorhombic (II) polymorphs of paracetamol. Axes of strain ellipsoids in the form I on cooling (T) and with increasing pressure (P) are shown, 1 – minimum, 2 – medium linear strain. In form II axis 1T is along **a**, 1P – along **a(b)**, 2T – along **b**, 2P – along **a(b)**. Hydrogen bonds are shown by red (OH...O) and blue (NH...O) lines.

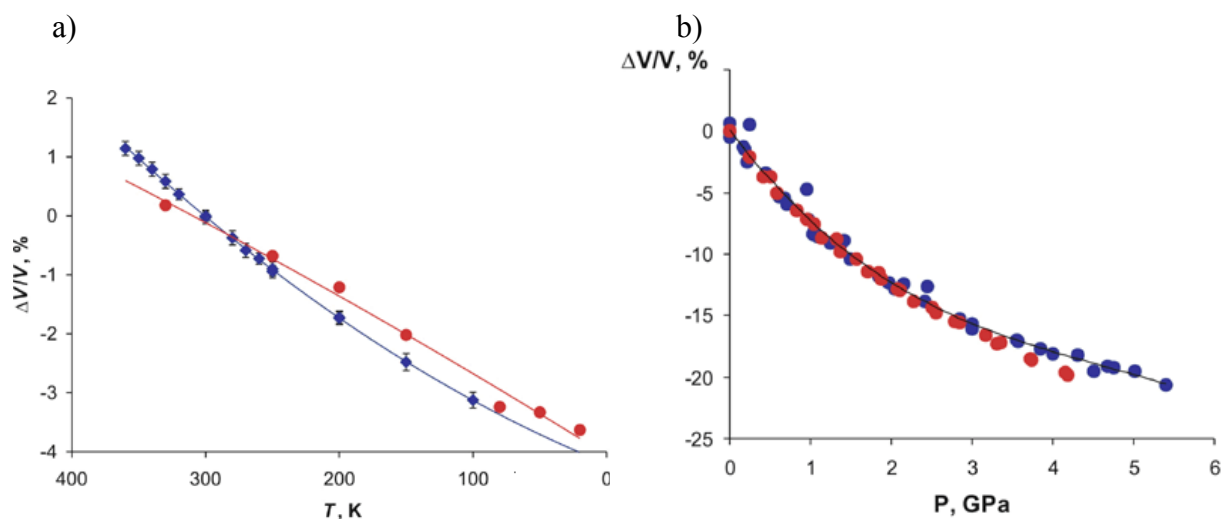
In order to induce a polymorphic transformation of one form of paracetamol into another, one would need to invert every second chain in a layer, breaking and re-making many hydrogen bonds. It seems natural, that such a transformation is kinetically hindered, and the range of conditions, under which a metastable form can exist, is much wider than could be expected. The

presence of water (or another potential solvent) facilitates re-crystallization, at least at the surface, and the nucleation of a new phase, and the transformation becomes possible. This effect was observed not only at variable-temperature, but also at variable-pressure conditions. When high pressure was applied to single crystals of the monoclinic polymorph I of paracetamol, no polymorphic transitions were observed at least till 4 GPa (the limit reached in the experiment).<sup>24</sup> However, if a powder sample of paracetamol I was subjected to hydrostatic compression, a polymorphic transition into the orthorhombic form II was observed at about 1.3 GPa. The transition was neither complete, nor fully reversible. Moreover, it was poorly reproducible and could be observed not on increasing pressure, but during a de-compression from a higher (4.2 GPa) pressure.<sup>23</sup> It is interesting, that polymorph II of paracetamol could be obtained as small single crystals, if paracetamol I was dissolved in a methanol-ethanol mixture and then compressed to 1.1 GPa.<sup>34</sup>

### Structural studies

The structural response of the two polymorphs of paracetamol to variations in pressure and temperature was followed by X-ray diffraction and IR-spectroscopy.<sup>8, 12, 13, 23-26, 37</sup> The aim of this study was to compare the anisotropy of lattice strain, to follow the intramolecular distortions and the changes in the intermolecular hydrogen bonds, to see if the anisotropy of structural strain can be correlated with the intra- and intermolecular distortions.

The isothermal bulk compressibility of the two polymorphs of paracetamol was practically the same within experimental error, whereas on cooling structural compression of the two polymorphs differed. The lattice strain of the monoclinic and of the orthorhombic polymorphs induced either by temperature changes,<sup>26,37</sup> or by increasing pressure<sup>23,24</sup> was shown to be noticeably anisotropic (Figure 6). The strain anisotropy was different for the volume decrease induced by cooling and by increasing pressure.



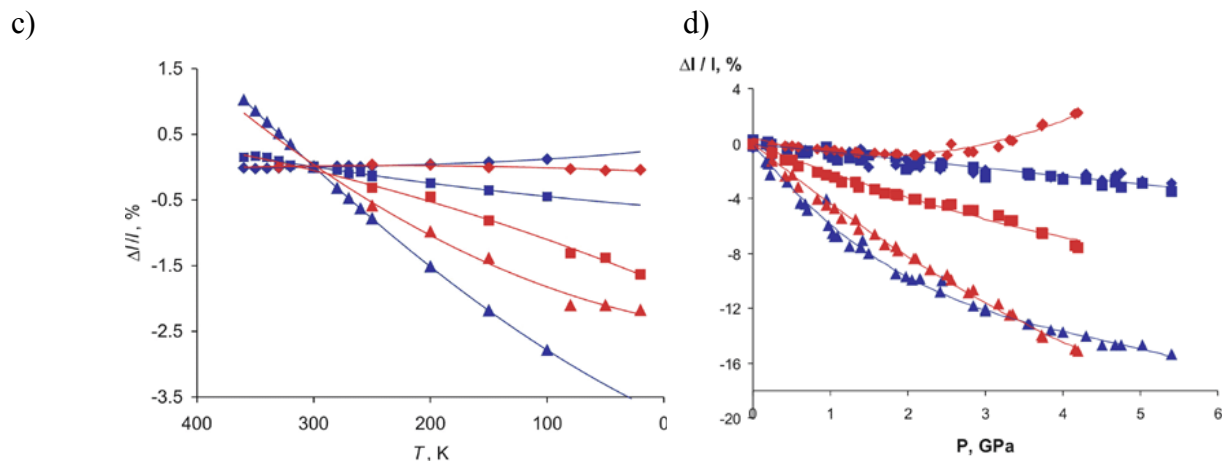


**Figure 6.** Relative volume changes (a,b) and linear strain along the principal axes of strain ellipsoids (c,d) in the monoclinic (red) and the orthorhombic (blue) polymorphs of paracetamol on cooling (a,c) and with increasing pressure (b,d).

On cooling, the interlayer compression in the orthorhombic form was larger, than in the monoclinic one. With increasing pressure, the interlayer compression in the two polymorphs was more similar. On cooling, a slight compression was measured in the orthorhombic form in the direction of the NH...O bonded molecular chains, and a slight expansion – along the direction of the OH...O bonded molecular chains (Figure 5, 6). Linear dimensions of molecules increased in this direction as the molecules got flatter. For the monoclinic paracetamol, the compression of the molecular layers on cooling was also anisotropic. A relatively large compression was observed in the direction close to the molecular chains linked via the NH...O bonds, and practically no linear strain – in the direction close to the OH...O bonds (Figure 5, 6).<sup>26,37</sup> For a comparison, with increasing pressure, the molecular layers of the orthorhombic paracetamol were compressed isotropically. With increasing pressure, the structure of the monoclinic polymorph expanded along the direction close to that of NH...O bonded molecular chains, and compressed in the direction close to that of the OH...O bonds (Figure 5,6).<sup>23,24</sup> With increasing pressure, the molecules of paracetamol got flatter, and the angle between the planes of the neighboring molecules in a layer also increased (Figure 7).



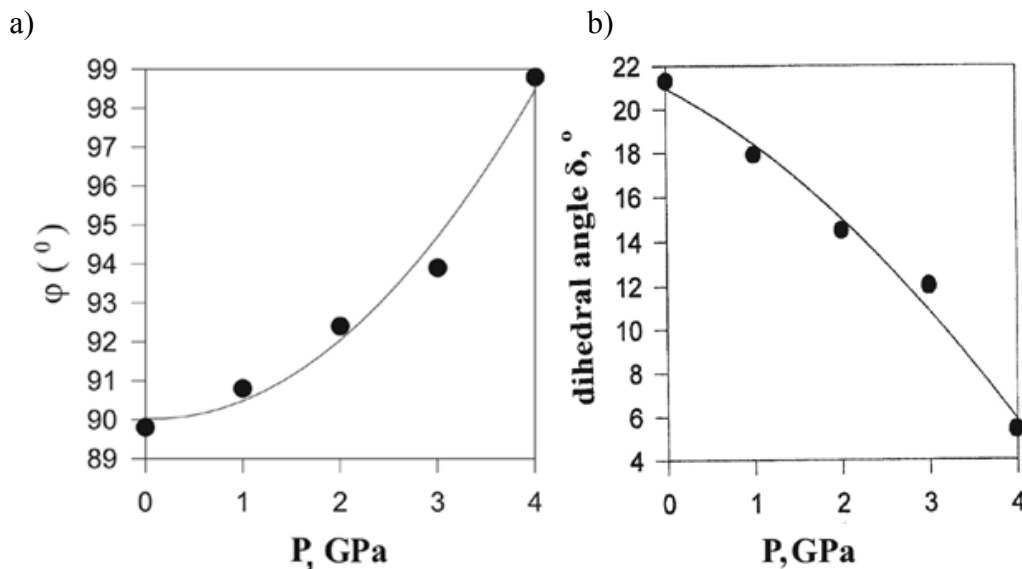


**Figure 7.** The dihedral angle between the planes of the phenyl ring and the acetamide group in a paracetamol molecule (a), and the angle between the planes of the phenyl rings of the two neighbouring molecules in a layer of the monoclinic polymorph (b) versus pressure.

The elongation of the  $\text{-C=O}$  bond, the change in the torsion angle, and the decrease in the values of the atomic displacement parameters on cooling and with increasing pressure are in an agreement with the shortening of the intermolecular  $\text{-OH}\dots\text{O(=C-)}$  and  $\text{-NH}\dots\text{O(H)-}$  hydrogen bonds<sup>24</sup>. Although the orthorhombic polymorph is denser, than the monoclinic one, the intermolecular hydrogen bonds (in particular – the  $\text{OH}\dots\text{O}$  bonds) can be supposed to be weaker in the orthorhombic form. They are longer in the orthorhombic form, than in the monoclinic one ( $\text{NH}\dots\text{O}$  by about 1%, or 0.4 Å,  $\text{OH}\dots\text{O}$  – by about 2%, or 0.6 Å). Besides, the stretching vibration  $\nu_{\text{OH}}$  is shifted to the red in the crystals of paracetamol as compared to the spectrum of an individual molecule, and the shift, which is assumed to correlate with the strength of a  $\text{OH}\dots\text{O}$  hydrogen bond, is by about  $40\text{ cm}^{-1}$  larger in the monoclinic polymorph, than the corresponding shift in the orthorhombic form<sup>25,38</sup>. On cooling, both in the monoclinic and in the orthorhombic polymorphs the longer  $\text{NH}\dots\text{O}$  bonds shorten more, than the shorter (and, presumably, stronger)  $\text{OH}\dots\text{O}$  bonds. The result is essentially different from the effect observed in the monoclinic form with increasing pressure, when the  $\text{NH}\dots\text{O}$  bonds are less compressible than the  $\text{OH}\dots\text{O}$  bonds, at least when the distance changes are already as large, as those at 1 GPa (the lowest pressure for which experimental data are available) (Figure 8)<sup>26</sup>. The larger expansion / contraction of the  $\text{NH}\dots\text{O}$  bonds as compared with that of the  $\text{OH}\dots\text{O}$  bonds on heating / cooling agrees well with the transformation between the polymorphic forms induced by temperature variation: the chains linked by the  $\text{OH}\dots\text{O}$  bonds are preserved in the two polymorphs, whilst a polymorphic transformation should involve breaking the  $\text{NH}\dots\text{O}$  bonds between these chains.

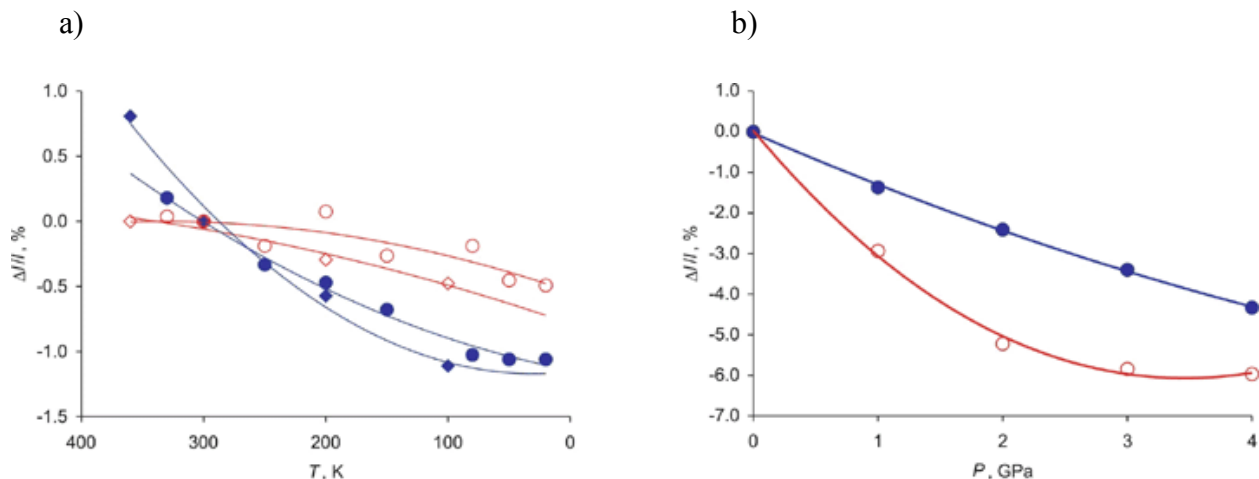


**Figure 8.** The distances between non-hydrogen atoms in the NH...O and OH...O hydrogen bonds in the two polymorphs of paracetamol on cooling (a) and with increasing pressure (b): circles – monoclinic form, rhombs – orthorhombic form; blue symbols – N1...O1, red symbols – O1...O2.

The flattening of the paracetamol molecules can be supposed to be interrelated with the compression of intermolecular hydrogen bonds, which manifests itself also in the IR-spectra.<sup>10,13,25</sup> According to *ab initio* calculations, an individual paracetamol molecule should be flat (torsion angle equal to 0),<sup>39</sup> but in the real crystal structures the torsion angle is equal to about 21°-23° in the monoclinic polymorph<sup>16,24</sup> and to about 18° in the orthorhombic form.<sup>15</sup> This can be explained by the effect of intermolecular hydrogen bonds formation on the torsion angle: *ab initio* calculations have shown the value of the torsion angle in the molecule to be sensitive to the protonation of the OH- and NH-groups.<sup>39</sup> The values of torsion angles in the paracetamol molecules differ in the two polymorphs,<sup>15,16,24</sup> in the various adducts formed by paracetamol with small organic molecules (in which some of the hydrogen bonds between the paracetamol molecules are broken and new hydrogen bonds are formed between the guest- and the paracetamol molecules, so that chains of paracetamol molecules are preserved),<sup>32,33</sup> in the paracetamol-methanol solvate (in which only short fragments of the chains are linked with each other via the methanol-bridges),<sup>34</sup> or in the paracetamol hydrates (in which the individual molecules of paracetamol are linked only via the H<sub>2</sub>O-bridges).<sup>35,36</sup>

The anisotropy of structural strain on cooling and with increasing pressure was often compared with the directions of weaker and stronger hydrogen bonds in the crystal structure. In the orthorhombic and in the monoclinic paracetamol, when discussing the anisotropy of structural strain, in addition to comparing the compressibility of the NH...O and OH...O hydrogen bonds, it is necessary to take into consideration the flattening of the molecules. Thus, the expansion of the structure of the orthorhombic paracetamol (on cooling), or of the monoclinic polymorph (with increasing pressure) in some directions cannot be explained without taking into account the changes in the torsion angles of the paracetamol molecules, since all the

intermolecular hydrogen bonds in the structures shorten (Figure 8). Correlations between the intramolecular conformational changes and the shortening in the intermolecular hydrogen bonds were observed also for several other molecular crystals.<sup>1-14</sup> The effect was more often reported for the structural distortions induced by variations in temperature, than for that with increasing pressure, but just because the data of the quality high enough to follow reliably intramolecular distortions can be obtained with much more efforts in the high-pressure experiments, than in the low-temperature ones.

### Polymorphs of glycine

The same phenomena as were observed when studying the polymorphs of paracetamol – the existence of the metastable polymorphs in a wide range of experimental conditions, different anisotropic response of a crystal structure to variations in temperature and pressure, the interplay between the intramolecular distortions and the changes in the network of the intermolecular hydrogen bonds in the crystal – are typical also for other molecular crystals. The crystals of amino acids are quite representative in this respect.

Glycine,  $\text{NH}_2\text{CH}_2\text{COOH}$ , is the simplest of all the amino acids (Figure 9). Three polymorphs were described for glycine at ambient pressure – two monoclinic forms ( $\alpha$ , s.gr.  $P2_1/n$ , and  $\beta$ , s.gr.  $P2_1$ ) and one trigonal form ( $\gamma$ , s.gr.  $P3_1$ ). The three polymorphs differ in the way how  $^+\text{NH}_3\text{-CH}_2\text{-COO}^-$  zwitter-ions are linked together in a hydrogen-bonds network. In the  $\alpha$ -polymorph zwitter-ions are linked via hydrogen bonds  $\text{NH}\dots\text{O}$  in double antiparallel layers, the interactions between these double layers being purely van-der-Waals. In the  $\beta$ -polymorph individual parallel polar layers are linked via hydrogen bonds in a three-dimensional network. In the  $\gamma$ -polymorph zwitter-ions form polar helices linked with each other via extra  $\text{NH}\dots\text{O}$  hydrogen bonds to give a three-dimensional polar network (Figure 10). In all the polymorphs, one can find the same structure-forming synthon – a head-to-tail chain of zwitter ions linked via bifurcated  $\text{NH}\dots\text{O}$  hydrogen bonds (Figure 11).<sup>40-44</sup>

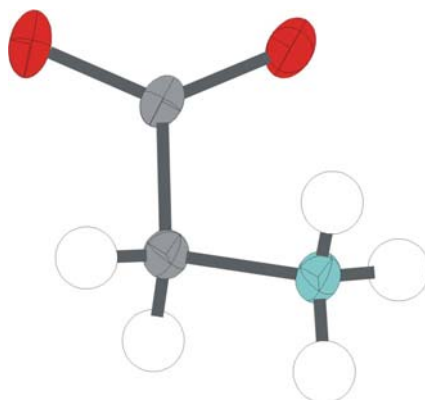


**Figure 9.** A zwitter-ion of glycine. Red – O, blue – N, grey – C, white – H.

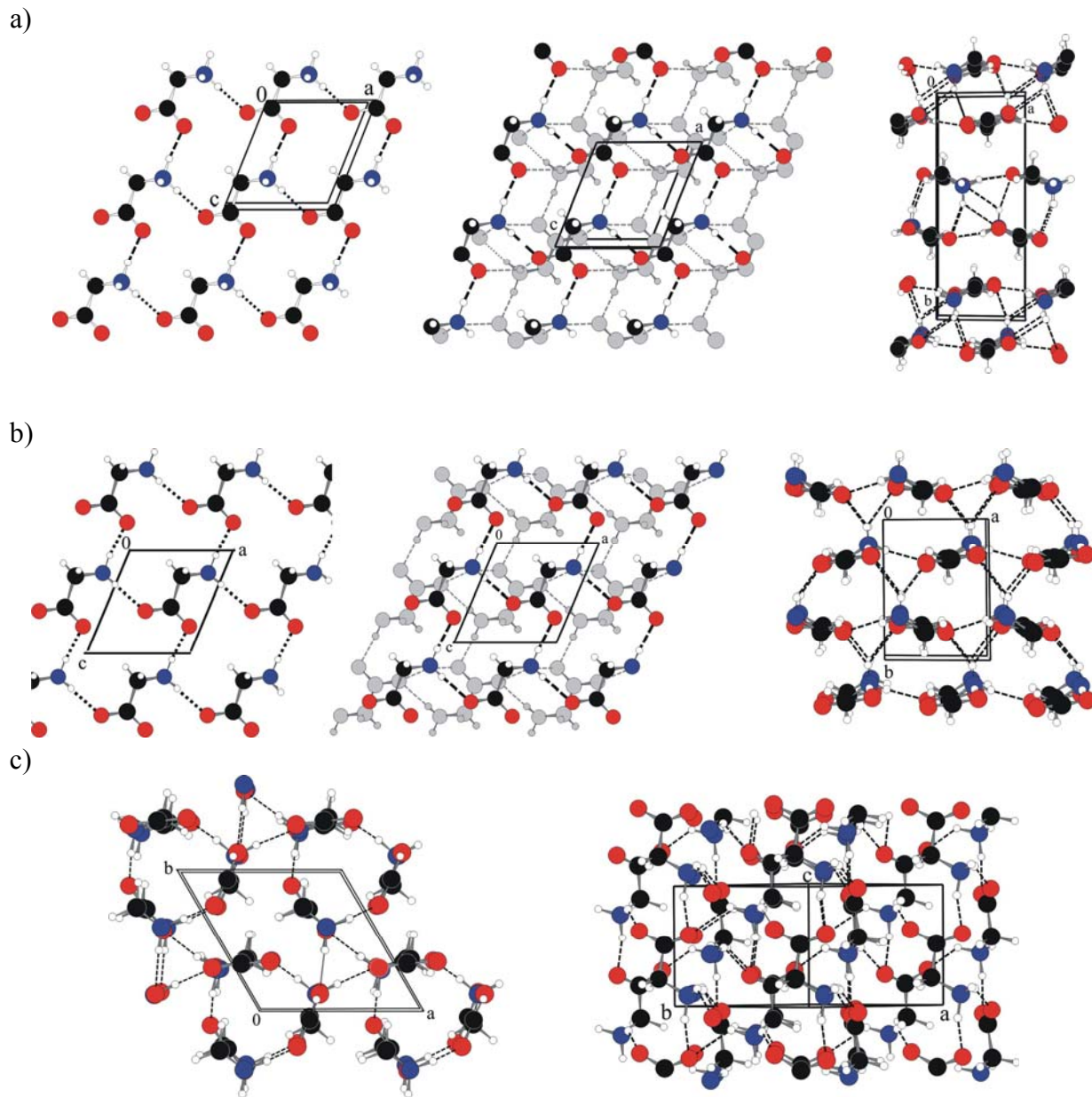


**Figure 10.** The fragments of crystal structures of the three polymorphs of glycine in two projections. Upper row – the  $\alpha$ -form (a), middle row - the  $\beta$ -form (b), lower row - the  $\gamma$ -form (c) of glycine; a,b - left – individual layers, middle – stacking of layers (all atoms coloured grey in the second layer), right – the fragments of the same polymorphs viewed in the projections normal to the layers; c – left - a view along the axes of the helices, right – a view normal to the axes of the helices.

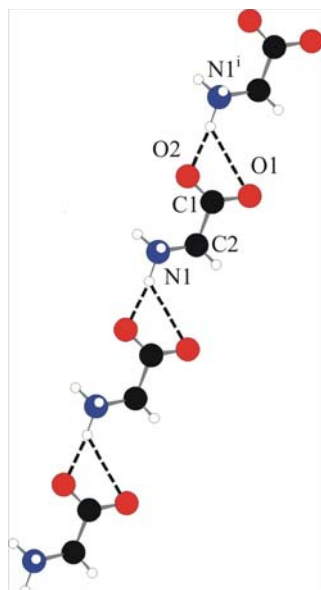


**Figure 11.** A head-to-tail chain formed by zwitter-ions of glycine.

### Crystallization and thermodynamic studies

The crystallization of glycine polymorphs is a remarkable illustration, that the relative stability of the polymorphs and the preferable growth of a particular polymorph in real experiments do not necessarily correlate directly. Moreover, the thermodynamic stability is not the same as the stability under particular storage conditions (in the presence of various gases/liquids in contact to the sample).

Thermodynamic stability can be characterized by a thermodynamic parameter – Gibbs energy. Enthalpy and entropy as functions of temperature that are required to calculate the Gibbs energy can be found experimentally from the measurements of heat capacity and the heats of transformations (such as heats of combustion, dissolution, or polymorphic transformation). Typically, temperature and pressure are considered to be the main parameters determining the thermodynamic parameters. For example, a thermodynamic stability can be determined for “ambient conditions” (pressure equal to 1 atm and temperature equal to 298.15 K). The composition of the gas phase providing this pressure is considered to be of less importance (if important at all). For many solids this is true. However, for the polymorphs of molecular crystals this assumption is no longer valid. The difference in the heats of formation and the heat capacities of the polymorphs can be so small, that heat fluctuations and a relatively small energy contribution from the interaction of the sample with the medium can result in a change in the free energy (Gibbs energy) exceeding the  $\Delta G$  between the polymorphs. This manifests itself in the calorimetric experiments (the difference in the thermodynamic functions measured for the polymorphs is within the experimental error even for the most accurate and precise measurements), in the experiments on crystal growth (concomitant polymorphs<sup>45</sup>), in the mutual transformations of the polymorphs on storage under various conditions. All this holds for the polymorphs of glycine<sup>46, 47</sup>.

The three forms of glycine usually crystallize simultaneously from the same solution,<sup>46,47</sup> that is they can be classified as concomitant polymorphs.  $\alpha$ -Polymorph crystallizes spontaneously under almost any experimental conditions; it is the main polymorph obtained from pure aqueous solutions. We have obtained the  $\alpha$ -form as an admixture to the  $\beta$ - and the  $\gamma$ -polymorphs as a result of crystallization from water solutions with additives of ethanol, ammonia, or acetic acid. At the same time, crystals of the  $\gamma$ - and the  $\beta$ - polymorphs were found as admixtures also in the samples crystallized from pure water and containing the  $\alpha$ -polymorph as the main product.

In many of the previously published papers the  $\alpha$ -polymorph was supposed to be the most stable form, since i) it is most easily obtained, ii) its transformation into the  $\gamma$ -form was not observed (the only two exceptions being the publication,<sup>48</sup> in which a moisture-mediated  $\alpha \rightarrow \gamma$  transformation was described, and the publication,<sup>43</sup> in which it was mentioned, that for deuterated  $\alpha$ -glycine (powder) the transformation from the  $\alpha$ - to the  $\gamma$ -form has actually been observed at room temperature).

The variable temperature measurements of the heat capacity of the glycine polymorphs made it possible to calculate the thermodynamic parameters, to estimate the order of relative stability of the polymorphs, and to calculate the changes in the enthalpy and the Gibbs free energy for the transitions between the polymorphs.<sup>46,47</sup> The order of the stability of the glycine polymorphs at ambient temperature was shown to be  $\gamma > \alpha > \beta$ . At 298.15 K,  $\Delta G$  for the  $\alpha$ - and the  $\gamma$ -forms was estimated as about 160 J/mol, predicting that the  $\gamma \rightarrow \alpha$  transition is thermodynamically forbidden at this temperature, whereas the reverse  $\alpha \rightarrow \gamma$  transition should be allowed. We did manage to initiate an  $\alpha \rightarrow \gamma$  transition at ambient temperatures using wet gaseous ammonia as a catalyst. At high enough temperatures the  $\gamma$ -form becomes less stable than the  $\alpha$ -form, and one can expect the  $\gamma \rightarrow \alpha$  transformation on heating, what is really the case. Our study<sup>46, 47</sup> has confirmed the hypothesis of Iitaka,<sup>43</sup> and of Sakai et al.,<sup>48</sup> that “the  $\gamma$  -form may be a stable form at least at room temperature”.

The order of stability  $\gamma > \alpha > \beta$  at ambient conditions found from our measurements correlates with the order of changes in the lattice energy calculated in<sup>49</sup> from the measured heats of dissolution of the three polymorphs in water. This correlation might seem obvious, but it is actually not. The same order in the lattice energy remains at the elevated temperatures, although the order of stability changes to  $\alpha > \gamma > \beta$ . Therefore, without calorimetric measurements, after the measurements of the heat of dissolution only, it was not possible to make a definite conclusion on the relative stability of the three polymorphs. Besides, the estimates of relative lattice energy cannot explain the conversion of the polymorphs into each other in the presence of various gasses. On storage in humid atmosphere,  $\gamma$ -glycine transforms into the  $\alpha$  -form. The same does the  $\beta$ -form. If, temperature and pressure being the same,  $\text{NH}_3$  and  $\text{H}_2\text{O}$  are present simultaneously in contact with a solid sample, a reverse transformation, that is from the  $\alpha$ -form into the  $\gamma$ -form is observed.  $\beta$ -Glycine also transforms into the  $\gamma$ -form under this conditions. In dry  $\text{NH}_3$  no polymorphous transitions take place, and any of the three polymorphs –  $\alpha$ -,  $\beta$ -, or  $\gamma$ - can be preserved during an indefinitely long time.<sup>46, 47</sup>

The differences in the Gibbs energies of the glycine polymorphs (Figure 12) are related to the differences in the weak intermolecular interactions. Therefore the heats of transitions between the polymorphs are rather low, and therefore the metastable forms can be obtained rather easily and can be preserved for a long time if the barriers required for a structural reorganization are much larger than the small potential energy gain resulting from the transformation.

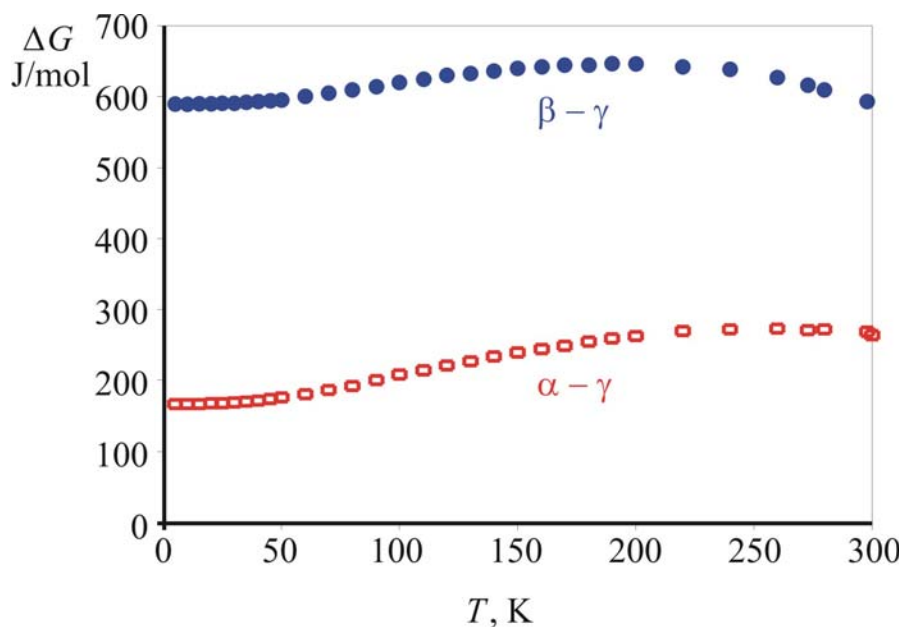


**Figure 12.** The difference in the Gibbs energy between the  $\alpha$ -, and the  $\gamma$ - polymorphs (red), and the  $\beta$ - and the  $\gamma$ -polymorphs (blue) versus T.

The relative stability of the polymorphs does not correlate directly with the easiness of their crystallization. The crystallization conditions, the structure of solution, and, first of all, the presence of pre-nuclei determine, which polymorph will grow. To induce crystallization of the  $\beta$  - or of the  $\gamma$ - polymorphs of glycine, it is necessary to destroy the dimers present in glycine solution,<sup>50</sup> which direct the crystallization towards the formation of the  $\alpha$ -form. This can be achieved by irradiating solutions with intense nanosecond pulses of near-infrared laser light,<sup>51, 52</sup> by changing solvents.<sup>40-43, 46-48, 50, and refs therein</sup> It is also possible to inhibit the growth of the  $\alpha$ -form, and in this way to stimulate the growth of the  $\gamma$ -form, by adding specially selected impurities (tailor-made additives) selectively binding to particular faces of a growing crystal,<sup>50, 53-58</sup> or by directing the nucleation using a Langmuir monolayer.<sup>50,59</sup> If the formation of the dimers in solution, and, hence, the growth of the  $\alpha$ -polymorph, is inhibited, then the stable  $\gamma$ -polymorph grows under crystallization conditions closer to the equilibrium (slow crystallization), whereas very quick precipitation gives the  $\beta$ -polymorph. It is also very important to exclude the presence of nuclei of undesirable polymorphs, and to introduce the nuclei of desirable polymorphs as precursors.<sup>46,47,50</sup> The fact that ageing of solutions is important for further crystallization can indicate that the clusters of glycine zwitterions in the solution keep memory of

their organization in the crystals prior to the dissolution. This effect was described previously for several other compounds.<sup>60, 61</sup> For  $\alpha$ -glycine, atomic-force microscopy (AFM) experiments on the growth and dissolution of single crystals have shown that a lower limit to the step size on the (010) glycine face is close to the thickness of the hydrogen-bonded bilayer, that is the dissolution of  $\alpha$ -glycine seems to proceed with preservation of dimers in solution. Diffraction data used together with the results of the *in situ* AFM measurements of glycine dissolution and growth in a complementary manner allow one to conclude that glycine leaves or docks to the crystal surface as cyclic hydrogen-bonded dimers.<sup>62-64</sup> One can suppose the clusters of glycine zwitter-ions keeping memory of the parent crystal structure to remain in solutions also after the dissolution of the  $\gamma$ -form. Since the chemicals used for the crystallization of glycine polymorphs never contain the  $\beta$ -form, but, generally, a mixture of the  $\alpha$ - and the  $\gamma$ -forms in different ratios, these two forms are also most easily crystallized from freshly prepared solutions – the  $\gamma$ -form if the formation of dimers is prevented, the  $\alpha$ -form - if not.

Isothermal cross-seeding experiments of suspensions with several polymorphs followed by monitoring the relaxation of the system (“slurry experiments”) are often applied to check the relative stability of the different forms.<sup>65, 66</sup> In the case of the polymorphs of glycine this procedure does not work well and gives poorly reproducible results. The reason is in the small difference in the stability of the three polymorphs, and in the strong effect of the structure of solution on the crystallization. The calorimetric experiments have proven to be really the best tool to range the glycine polymorphs according to their stability as solids, independently from the interactions with solvent.

### Structural studies

Comparative variable-temperature / variable-pressure studies of the glycine polymorphs have revealed interesting phenomena. On cooling, no phase transitions, but only the continuous anisotropic structural distortion could be detected for the glycine polymorphs by X-ray diffraction<sup>44</sup>, although for the  $\beta$ - and the  $\gamma$ -form low-temperature phase transitions, presumably of piezoelectric nature, were detected by calorimetry (Figure 13).<sup>46,47</sup> A piezoelectric phase transition in these systems seems not to affect noticeably the cell parameters and volume, as well as the coordinates of non-hydrogen atoms. Relatively small shifts of hydrogen atoms would be difficult to detect by X-ray diffraction. Low-temperature Raman spectroscopy has recently confirmed the existence of low-temperature phase transition in the  $\beta$ -glycine.<sup>67</sup> Interestingly, a  $\beta$   $\alpha$  polymorphous transition could be induced by repeated temperature cycling in the vicinity of the low-temperature piezoelectric phase transition in the  $\beta$ -form.<sup>46, 47</sup>



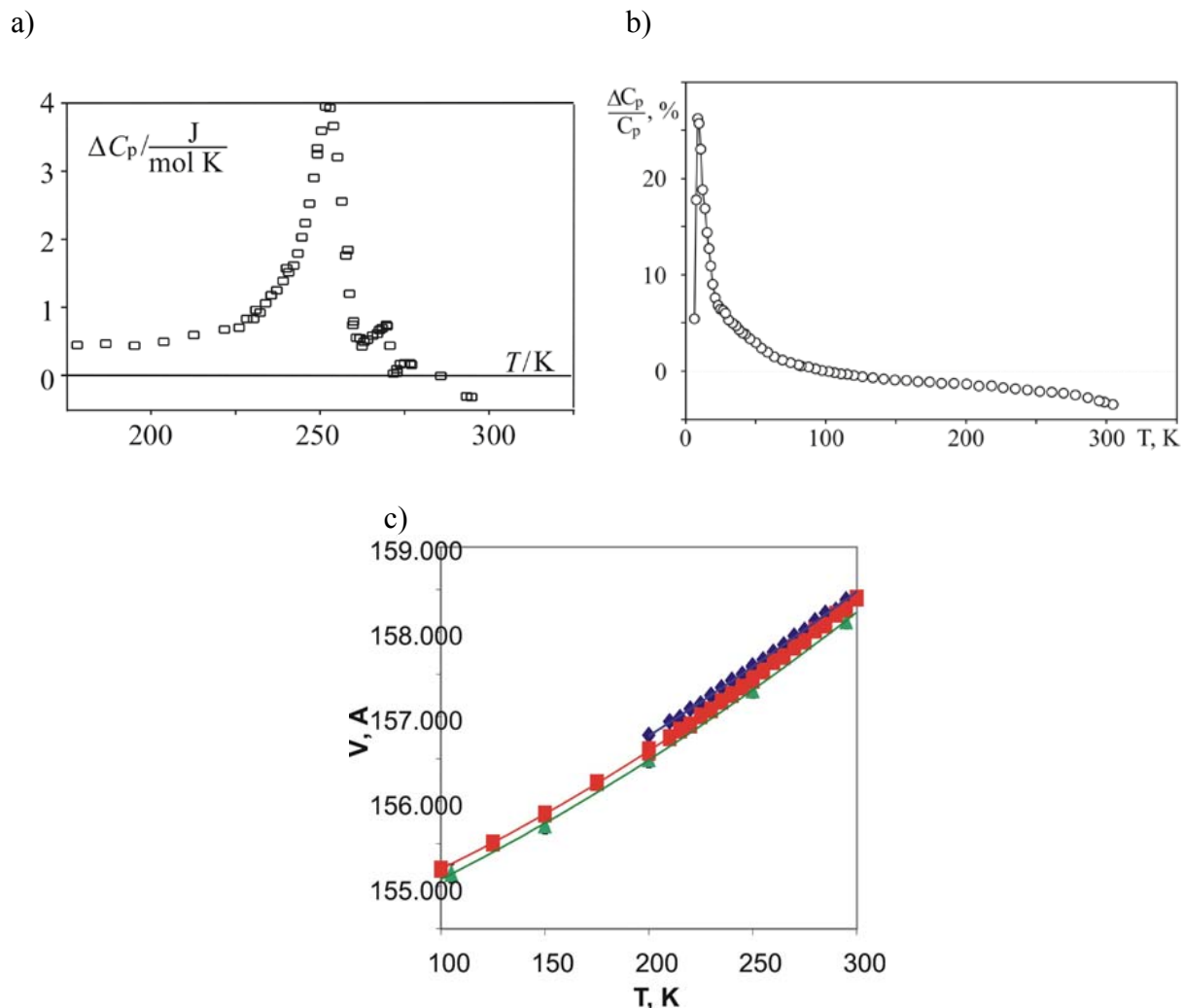
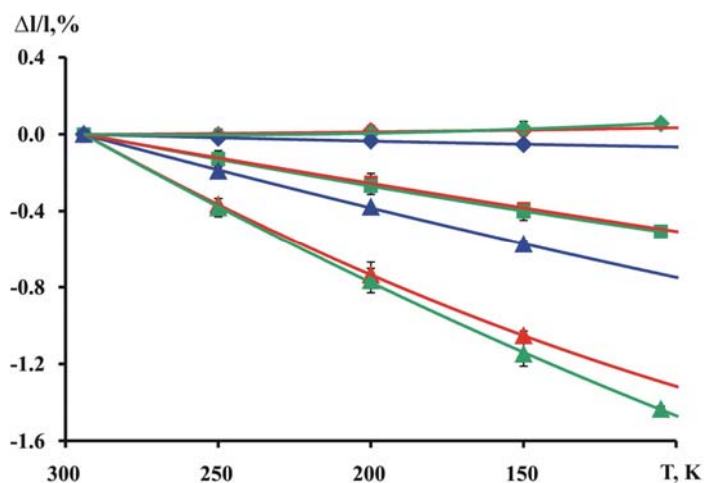


**Figure 13.** Heat-capacity peaks at low-temperature phase-transitions in the  $\gamma$ -glycine (a) and in the  $\beta$ -glycine (b); the changes in the cell volume of the  $\beta$ -glycine in the temperature range near the phase transition (different colour corresponds to different crystals) (c).

The directions of maximum and minimum lattice strain were related to the directions of weak and strong hydrogen bonds in the structures. On cooling, minimum compression (in the  $\gamma$ -polymorph) and even a slight expansion (in the  $\alpha$ - and the  $\beta$ -polymorphs) was measured in the direction of the head-to-tail hydrogen-bonded chains of zwitter-ions. Maximum compression of the structures of the glycine polymorphs was measured in the directions normal to the triple helices formed by the chains (in the  $\gamma$ -polymorph), or to the layers, in which the chains were linked with each other via extra NH...O bonds (Figure 11, 14). Expansion of the crystal structure in particular directions (in the  $\alpha$ - and  $\beta$ -polymorphs) was related not only to the distortion of the NH...O hydrogen bonds, but, first of all, to the distortions in the torsion angles within glycine zwitter-ions. This effect was even more pronounced, when the effect of cooling on the simplest dipeptide, glycylglycine and its hydrate, was considered. The structure of glycylglycine expanded

on cooling along the direction of molecular axes coinciding also with the direction of the shortest NH...O intermolecular hydrogen bonds. The linear strain in glycylglycine was larger than in any polymorph of glycine (Figure 15).<sup>68</sup> In glycylglycine hydrate, the relative volume change on cooling is slightly larger, than that in glycylglycine. However, it would be erroneous to consider the structure of glycylglycine to be more compressible than that of glycylglycine: linear strain in the directions of principle axes is smaller in glycylglycine hydrate, than in glycylglycine (Figure 15).

a)



b)

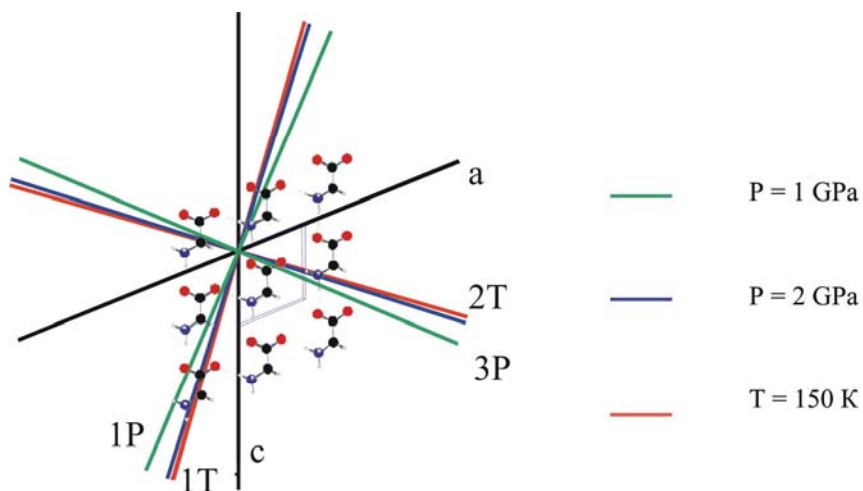


**Figure 14.** Linear strain along the principal axes of strain ellipsoids of the  $\alpha$ -form (red),  $\beta$ -form (green), and the  $\gamma$ -form (blue) of glycine on cooling (a) and the orientation of the principal axes of strain ellipsoid on cooling (1T, 2T, red) and with increasing pressure (1P, 2P, green, blue) with respect to the crystallographic axes in the  $\alpha$ - and  $\beta$ -forms (b); in the  $\gamma$ -form minimum strain is along c, maximum – in the plane normal to c.<sup>44</sup>

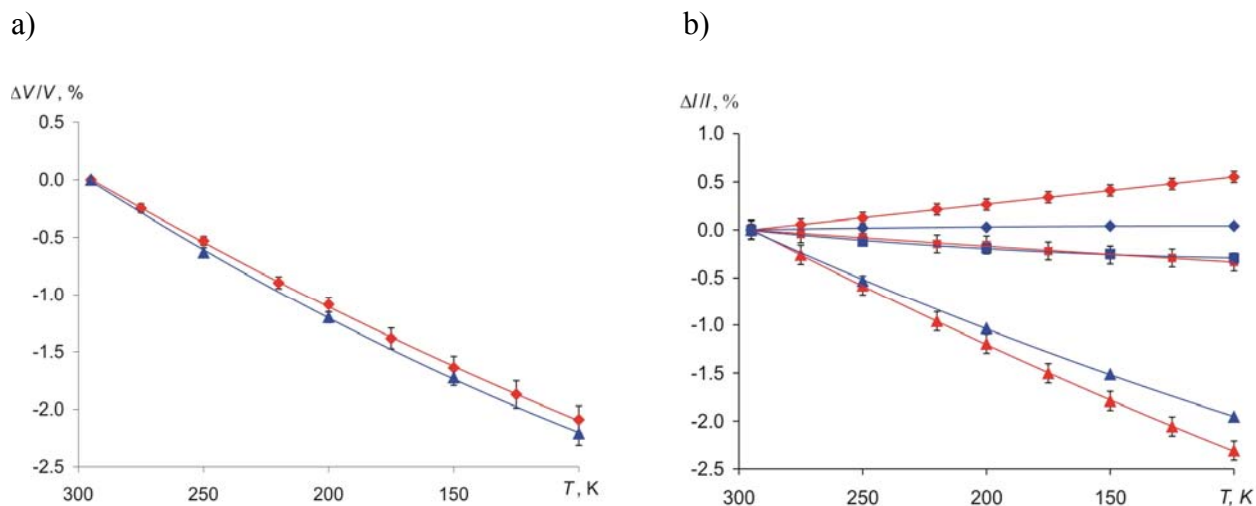


**Figure 15.** Relative volume changes (a) and linear strain along the principal axes of strain ellipsoids (b) of the  $\alpha$ -glycylglycine (red) and the  $\alpha$ -glycylglycine hydrate (blue) on cooling.

The response of the polymorphs of glycine to increasing pressure is remarkably different. No polymorphic transitions were observed when applying pressure up to 4 GPa (X-ray diffraction),<sup>69</sup> or 23 GPa (Raman spectroscopy)<sup>70</sup> to  $\alpha$ -glycine, and the anisotropy of structural strain was not the same as the one induced by cooling (Figure 10, 16).<sup>44,69</sup> A reversible phase transition in the  $\beta$ -polymorph was observed by Raman spectroscopy at about 0.76 GPa.<sup>71,72</sup> The structure of  $\gamma$ -glycine was shown to undergo a partly reversible polymorphic transformation into a previously unknown polymorph of glycine, the  $\delta$ -form (the structure of which was successfully solved and refined in the Pn space group), in a wide pressure range between 2.7 GPa and 7.8 GPa. On decompression, the high-pressure phase did not disappear completely even at ambient pressure. At about 3.3 GPa the amount of the initial  $\gamma$ -polymorph started to increase noticeably. When pressure reached 0.2 GPa, some additional lines appeared, that could not be assigned either to the high-pressure polymorph, or to the  $\gamma$ -glycine, to the  $\alpha$ -, or to the  $\beta$ -phases of glycine.<sup>73, 74</sup>

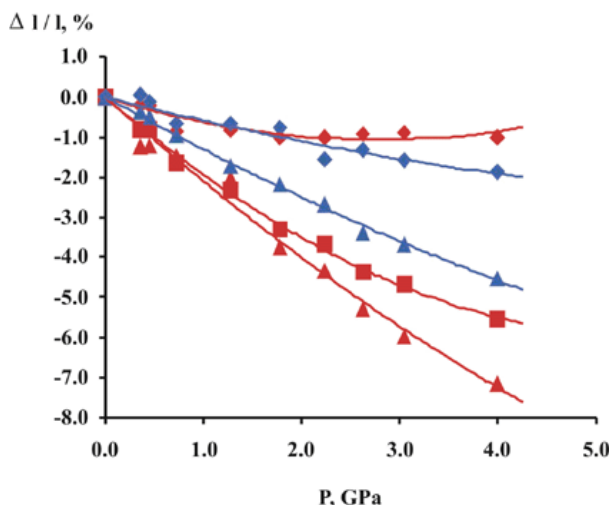


**Figure 16.** Linear strain along the principal axes of strain ellipsoids of the  $\alpha$ - form (red) and the  $\gamma$ -form (blue) of glycine with increasing pressure (the orientation of the principal axes of strain ellipsoid with respect to the crystallographic axes in the  $\alpha$ - form see in Figure 14b; in the  $\gamma$ -form minimum strain is along  $c$ , maximum – in the plane normal to  $c$ ).<sup>69</sup>

The structural “synthone” – a chain of zwitter-ions, that is present in the three previously known polymorphs of glycine ( $\alpha$ -,  $\beta$ -, and  $\gamma$ -) – is present also in the structure of the high-pressure  $\delta$ -form. The chains of the glycine zwitter-ions are, in turn, linked via additional hydrogen bonds with each other to give not the helices, as in the original  $\gamma$ -glycine, but layers, similar to those in the  $\alpha$ - and  $\beta$ - forms. The stacking of the layers in the  $\delta$ -form is essentially different from those in the  $\alpha$ -, and in the  $\beta$ -polymorphs: the layers in the  $\delta$ -polymorph are double, as in the  $\alpha$ -form, but the individual layers in the double-layer band are not related with each other by inversion, as in the  $\alpha$ -form, but solely by a glide plane, so that the structure of the  $\delta$ -form remains polar, as the structure of the parent  $\gamma$ -form was (Figure 17).<sup>73,74</sup> It is remarkable, that the distortion of the chains of zwitter-ions in the  $\gamma$ - and in the  $\delta$ -polymorphs was continuous in all the pressure range from ambient to 7.85 GPa, despite a polymorphic transformation (Figure 18).

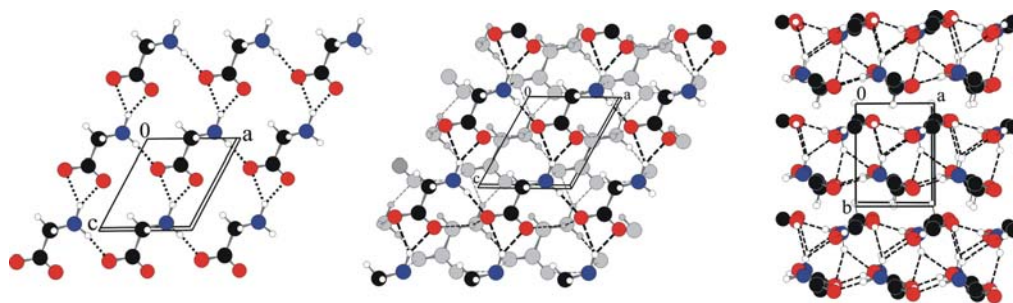


**Figure 17.** A fragment of the crystal structure of the high-pressure  $\delta$ -polymorph of glycine; a – an individual layer, b – stacking of layers, c – a view normal to the layers.

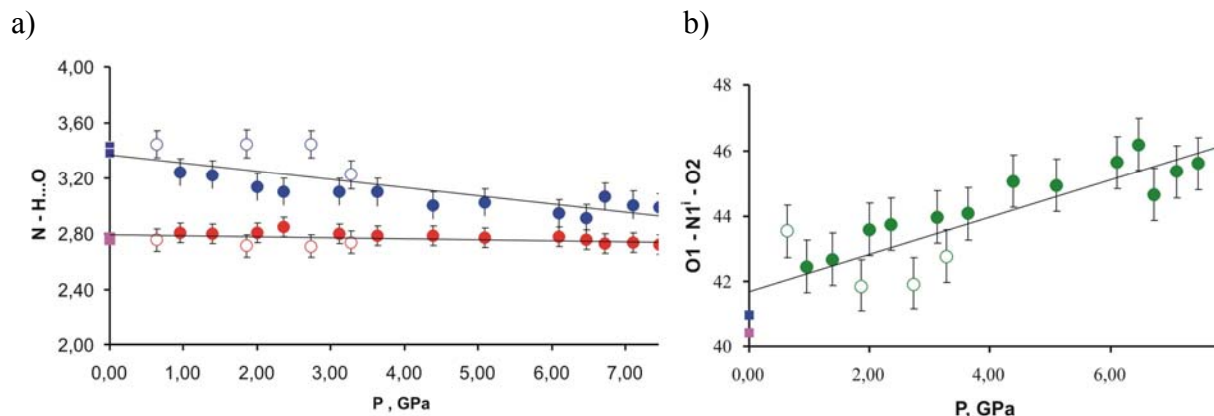


**Figure 18.** The changes in the selected distances and angles within a chain in the starting  $\gamma$ - and in the new high-pressure  $\delta$ -polymorphs of glycine versus pressure: (a) the distances N-O in the NH...O hydrogen bonds; (b) the O1-N1<sup>i</sup>-O2 angle. Open symbols –  $\gamma$ -polymorph, filled symbols –  $\delta$ -form.

Although the chains of zwitter-ions in the  $\delta$ -polymorph form layers similar to those in the  $\alpha$ -form, the  $\delta$ -polymorph could be formed when applying pressure not to the  $\alpha$ -polymorph, but to the  $\gamma$ -polymorph, in which such layers are not present, but can be formed from linked chains of zwitter-ions aligned parallel to the crystallographic c-axis if part of the zwitter-ions rotate with respect to each other along the chain axis. This transformation seems to be kinetically hindered (is observed in a wide pressure range and is not completely reversible on decompression). Piezoelectric properties of the  $\gamma$ -glycine<sup>42</sup> can be supposed to be important for the mechanism of the  $\gamma \rightarrow \delta$  transformation: electric field induced in the crystal by applying hydrostatic pressure may influence on the reorientation of the dipoles of zwitter-ions. It is interesting, that another glycine polymorph that undergoes a phase transition under pressure, the  $\beta$ -form, is also piezoelectric.<sup>42</sup>

### L-serine and D,L-serine

The pressure-induced polymorphic transformation in the  $\gamma$ -polymorph can be compared with a change in the secondary structure of a polypeptide chain from a helix into a layer.<sup>73,74</sup> Detailed studies of the response of the polymorphs of crystalline amino-acids to increasing pressure can be helpful to achieve a better understanding of the effect of pressure on peptides. In particular, the compressibility of the hydrogen bonds, or the flexibility of torsion angles can be compared and correlated with the “softness” of a structure along selected directions. In addition, for all the amino acids but glycine, the behaviour of L-compounds can be compared with that of D,L-racemates.

As an example, the structural response of crystalline serine to cooling and to increasing pressure can be considered.

The crystal structure of L-serine is formed by zwitter-ions (Figure 19) linked via NH...O hydrogen bonds into "head-to-tail" chains along the crystallographic axis **a**, similar to those in the polymorphs of glycine. Every NH<sub>3</sub>-group in the chain forms two NH...O hydrogen bonds with the neighbouring carboxyl group: a short bond with one oxygen atom (bond 1) and a long bond with another oxygen atom (bond 2). The chains of zwitter-ions of L-serine are linked via extra NH...O hydrogen bonds into a 3D-network. In the plane (**a** × **b**), the neighbouring chains are antiparallel to each other and are linked by the hydrogen bonds NH...O along **b** (bond 3). In the plane (**a** × **c**), the neighbouring chains of the zwitter-ions are parallel to each other and are related by a 2<sub>1</sub> screw axis parallel to axis **a**. Every chain is linked to one neighbouring chain in the plane via NH...O hydrogen bonds (bond 4 along **c** axis) and with another neighbouring chain via OH...O bonds between the side CH<sub>2</sub>OH groups (bond 5 along axis **a**) (Figure 20).<sup>75-77</sup>

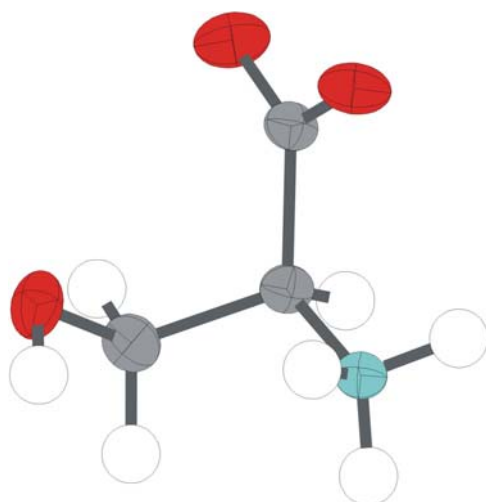


**Figure 19.** A zwitter-ion of serine.

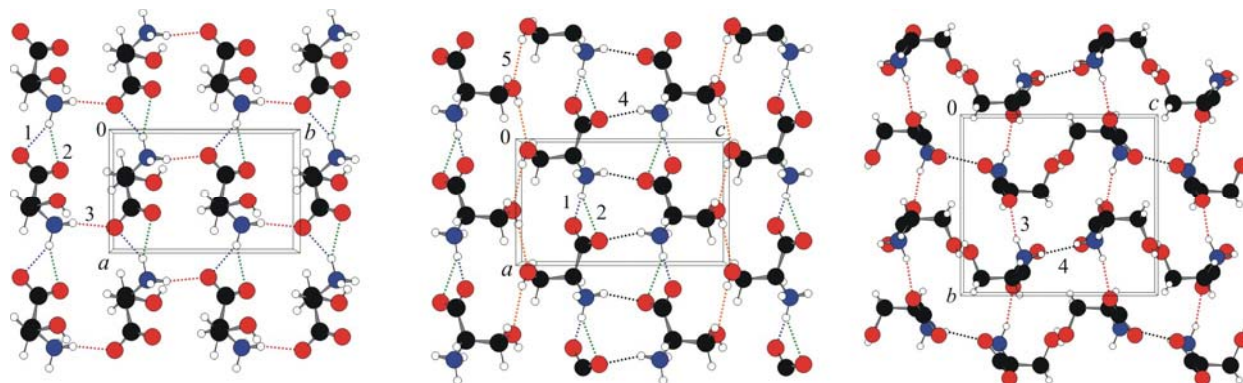


**Figure 20.** The fragments of crystal structure of L-serine.

The directions of the principal axes of strain ellipsoids on cooling and with increasing pressure coincide with the **a**, **b**, and **c** crystallographic directions in the structure of L-serine and

can be correlated with the structure of the NH...O and OH...O hydrogen bond network (Figure 20, 21). The most rigid (both on cooling and with increasing pressure) direction in the structure of L-serine is the direction along axis **a**, corresponding to the shortest cell parameter. It coincides with the direction of the "head-to-tail" chains formed by serine-zwitter-ions (Figure 20). The structures of all the polymorphs of glycine, and of L-alanine were also reported to have the minimum linear strain in the directions of these chains on cooling (the structures of  $\alpha$ -glycine,  $\beta$ -glycine, L-alanine expand slightly in these directions with decreasing temperature).<sup>77</sup> For the  $\alpha$ -,  $\gamma$ -, and  $\delta$ -glycine the directions of these chains were shown to be the most rigid also when applying pressure to the samples.<sup>69, 73, 74</sup> With increasing pressure, the structure of  $\alpha$ -glycine first compresses slightly and then starts to expand in the direction of the "head-to-tail" chains.<sup>69</sup> The structure of L-serine expands along these chains on cooling and compresses with increasing pressure.<sup>77</sup>

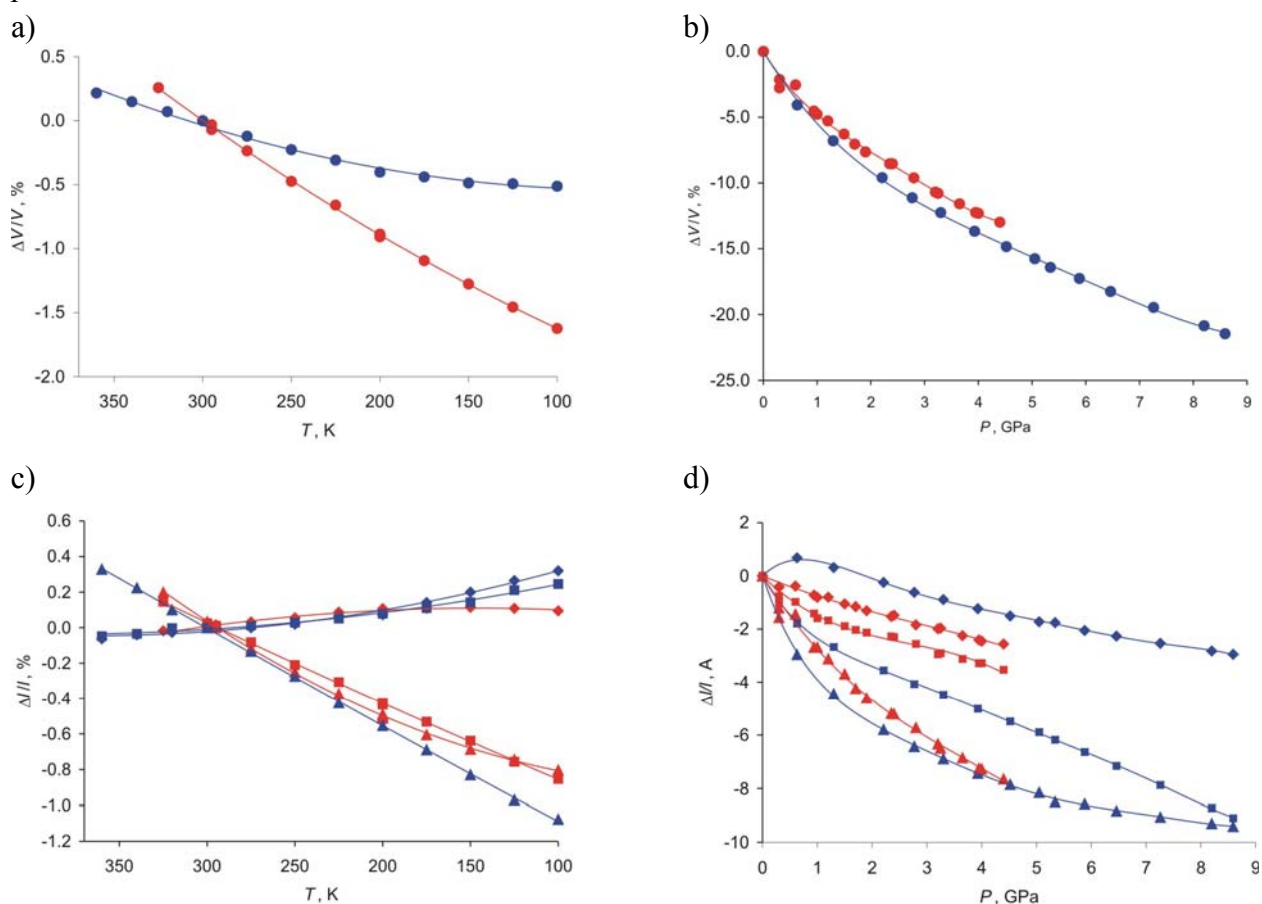


**Figure 21.** Relative changes in cell volume (a,b) and linear strain along the principal axes of strain ellipsoids (c,d) in L-serine (red) and D,L-serine (blue) on cooling (a,c) and with increasing pressure (b,d).

The compression of the structure of L-serine along axis **b** on cooling is comparable with that along axis **c**. In contrast to that, with increasing pressure the same structure compressed noticeably less along **b** direction, than along **c** axis (Figure 21). The different anisotropy of

lattice strain of the same structure on cooling and under pressure is remarkable. Earlier, the striking differences in anisotropy of structural strain on cooling and with increasing pressure were reported for Co(III) nitroammine complexes,<sup>78-80</sup> and the polymorphs of paracetamol.<sup>23-26</sup> The anisotropy of strain on cooling and with increasing pressure was not the same also for sodium oxalate,<sup>81</sup> or the  $\alpha$ - polymorph of glycine.<sup>44,69</sup> In the  $\alpha$ -glycine the most rigid (and even slightly expanding) direction in the structure is the same for the strain induced by cooling and by increasing pressure (along the "head-to tail" chains). At the same time, with increasing pressure the largest compression of the structure was observed in the plane of the layers formed by glycine zwitter-ions, in the direction of the bonds linking the "head-to tail" chains with each other to form a layer. On cooling, the same structure was most compressible in the direction normal to these planes. The difference between the compressibility within a molecular layer and in the direction normal to it was rather small with increasing pressure, but quite pronounced - on cooling. For the  $\gamma$ -glycine, however, the anisotropy of strain on cooling and with increasing pressure was similar.<sup>44,69</sup> Very similar structural distortion on cooling and with increasing pressure was reported for 1,3-cyclohexanedione.<sup>82,83</sup> The different response of the same structure to cooling and to increasing pressure may be caused by a different relative compressibility of the different types of hydrogen bonds in the same structure. The changes in the conformations of molecules should be also taken into account.

The behavior of the crystal structure of L-serine on cooling and with increasing pressure was very different from that of D,L-serine. On cooling, the structure of D,L-serine is noticeably less compressible than that of L-serine, if one considers the relative volume changes (Figure 21). The anisotropy of structural distortion is also remarkably different: the structure of D,L-serine expands on cooling in many crystallographic directions, whereas in the structure of L-serine compression on cooling prevails (Figure 21). With increasing pressure, the difference between the L- and the D,L-serine is even larger. The relative volume changes in the L- and D,L-serine are very similar up to about 4 GPa, but then the crystal structure of L-serine undergoes a phase transition at about 4-5 GPa, as recently shown by Raman spectroscopy measurements.<sup>84</sup> The transition was observed at 5.3 GPa when the sample was compressed, and at 4.5 GPa on decompression at ambient temperature. D,L-serine showed no phase transitions at least up to 8.6 GPa (the maximum pressure reached in the experiment), as recently shown by high-pressure single-crystal X-ray diffraction.<sup>85</sup> The anisotropy of strain with increasing pressure was very different in L- and in D,L-serine (Figure 21).<sup>86</sup> The striking difference in the behavior of L- and D,L-serine on cooling and with increasing pressure could be related to the differences in the two crystal structures, in general, and in the structure of the hydrogen bond networks, in particular.<sup>85</sup>

## Conclusions

We hope to have demonstrated at several examples from our own practice, that variable-temperature and variable-pressure studies can be helpful for understanding the structural and thermodynamic features of the small-molecule organic crystals. They can be used for studying



the relative stability of the polymorphs, for finding the conditions of polymorphic transitions, for understanding the nature of the metastability of the polymorphs. They can be also very useful for studying the intermolecular interactions in the molecular crystals and their interrelation with the changes in the intramolecular geometry, mutual orientation of molecules, and the macroscopically observed anisotropy of structural strain.

## Experimental Section

**General Procedures.** The general procedures and equipment were described in details in the original publications.<sup>13, 23-27, 46, 47, 67-69, 71-74, 77-81, 84, 85</sup> High pressure was created in the diamond anvil cells of various types. The temperature was controlled with a 600 Series Cryostream Cooler (Oxford Cryosystem). X-ray diffraction experiments were carried out using powder and single-crystal techniques, also with synchrotron radiation source at the Swiss-Norwegian Beam Line at ESRF (Grenoble).

**Compound characterization.** The procedures for the preparation and the characterization data for compounds used were described in details in the original publications.<sup>13, 23-27, 46, 47, 67-69, 71-74, 77-81, 84, 85</sup>

## Acknowledgements

The study was supported by RFBR (grants 02-03-33358 and 02-05-65313), the BRHE-Program (grant NO-008-XI), Russian Ministry of Education (grants Ч0069 of the “Integration”-Program; 3H-67-01; and yp.05.01.021 of the Program “Universities of Russia”); Humboldt Foundation, DFG, DLR (Germany); the Russian National Science Support Foundation for EVB (Program “Young Professors”); CRDF Support of Young Scientists (SNI). The diffraction experiments using synchrotron radiation were carried out at the Swiss-Norwegian Beamline (SNBL) at ESRF (Grenoble), experiments 01-02-656 и 01-02-671. The assistance of the SNBL-team is gratefully acknowledged.

## References and Footnotes

1. Katrusiak, A. *Cryst. Res. Technol.* **1991**, *26*, 523.
2. Katrusiak, A. *Phys. Rev. B* **1993**, *48*, 2992.
3. Katrusiak, A. *Phys. Rev. B* **1995**, *51*, 589.
4. Katrusiak A. *Crystallogr. Rev.* **1996**, *5*, 133.
5. Hemley, R. J.; Dera, P. *Molecular crystals. Rev. Mineral. Geochem. Soc. America* **2000**, *41*, 335.

6. Katrusiak, A. In *Frontiers of High-Pressure Research*; Hochheimer, H.D.; Kuchta, B.; Dorhout, P.K.; Yager, J. L. Eds.; Kluwer Academic Publishers: Dordrecht, Boston, London, 2001; pp 73-85.
7. Katrusiak, A. *Crystallogr. Rev.* **2003**, 9, 91.
8. Boldyreva, E.V. *J. Molec. Struct.* **2003**, 647, 159.
9. Katrusiak, A.; McMillan, P. Eds.; *High-Pressure Crystallography; NATO Science Series, II. Mathematics, Physics*; Kluwer: Dordrecht, Chemistry, 2004; p 140.
10. Boldyreva, E. V. In *High-Pressure Crystallography*; Katrusiak, A.; McMillan, A. Eds.; *NATO Science Series, II. Mathematics, Physics, Chemistry*; Kluwer: Dordrecht, 2004, 140, pp 495-512.
11. Katrusiak, A. In *High-Pressure Crystallography*, Katrusiak, A.; McMillan, P. Eds.; *NATO Science Series, II. Mathematics, Physics, Chemistry*; Kluwer: Dordrecht, 2004, Vol. 140, pp 513-520.
12. Boldyreva, E.V. *J. Molec. Struct.* **2004**, 700, 151.
13. Boldyreva, E.V. *Cryst. Engineer.* **2004**, 6/4, 235.
14. Boldyreva, E.V. *Russ. Chem. Bull.* **2004**, 53/7, 1315.
15. Haisa, M.; Kashino, S.; Maeda, H. *Acta Crystallogr.* **1974**, B30, 2510.
16. Haisa, M.; Kashino, S.; Kawai, R.; Maeda, H. *Acta Crystallogr.* **1976**, B32, 1283.
17. DiMartino, P.; Conflant, P.; Drache, M.; Huvenne, J.-P.; Guyot-Hermann, A.-M. *J. Therm. Analys. Calorim.* **1997**, 48, 447.
18. Peterson, M.L.; Morissette, S.L.; McNulty, C.; Goldsweig, A.; Shaw, P.; LeQuesne, M.; Monagle, J.; Encina, N.; Marchionna, J.; Johnson, A.; Gonzalez-Zujasti, J.; Lemmo, A.V.; Ellis, S.J.; Cima, M.J.; Almarsson, O. *J. Amer. Chem. Soc.* **2002**, 124, 10958.
19. Beyer, T.; Day, G.M.; Price, S.L. *J. Amer. Chem. Soc.* **2001**, 123, 5086.
20. Nichols, G.; Frampton C.S. *J. Pharm Sci.* **1998**, 87, 684.
21. Di Martino, P.; Guyot-Hermann, A.-M.; Conflant, P.; Drache, M.; Guyot, J.-C. *Int. J. Pharm.* **1996**, 128, 1.
22. de Wet, F.N.; Gerber, J.J.; Lötter, A.P.; van der Watt, J.G.; Dekker, T.G.; *Drug. Devel. Industr. Pharm.* **1998**, 24, 447.
23. Boldyreva, E.V.; Shakhtshneider, T.P.; Ahsbahs, H.; Sowa, H.; Uchtmann, H. *J. Therm. Anal. Calorim.* **2002**, 68, 437.
24. Boldyreva, E.V.; Shakhtshneider, T.P.; Vasilchenko, M.A.; Ahsbahs, H.; Uchtmann, H. *Acta Crystallogr.* **2000**, B56, 299.
25. Boldyreva, E.V.; Shakhtshneider, T.P.; Ahsbahs, H.; Uchtmann, H.; Burgina, E.B.; Baltakhinov, V.P. *Polish J. Chem.* **2002**, 76, 1333.
26. Drebushchak, T.N.; Boldyreva, E.V. *Z. Kristallogr.* **2004**, 21/8, 506.
27. Boldyreva, E.V.; Drebushchak, V.A.; Paukov, I.E.; Kovalevskaya, Yu.A.; Drebushchak, T.N. *J. Therm. Analys. Calorim.* **2004**, 77, 607.
28. Mikhailenko, M. *J. Cryst. Growth* **2004**, 265, 616.

29. Drebuschak, V.A.; Boldyreva, E.V.; Drebuschak, T.N.; Shutova, E.S. *J. Cryst. Growth*, **2002**, *241*, 266.
30. *Large Encyclopedic Dictionary. Physics*, Scientific Publishing House Large Russian Encyclopedia: Moscow, 1998; p 749.
31. Desiraju, G. *Angew. Chem.* **1995**, *107*, 2541.
32. Oswald, I.D.H.; Allan D.R.; McGregor, P.A.; Motherwell, W.D.S.; Parsons, S.; Pulham, C.R. *Acta Crystallogr.* **2002**, *B58*, 1057.
33. Oswald, I.D.H.; Motherwell, W.D.S.; Parsons, S.; Pulham, C.R. *Acta Crystallogr.* **2002**, *E58*, 1290.
34. Fabbiani, F.P.A.; Allan, D.R.; David, W.I.F.; Moggach, S.A.; Parsons, S.; Pulham, C.R. *Cryst. Engineer. Commun.* **2004**, *1*.
35. Parkin, A.; Parsons S.; Pulham, C.R. *Acta Crystallogr.* **2002**, *E58*, 1345.
36. McGregor, P.A.; Allan, D.R.; Parsons, S.; Pulham, C.R. *J. Pharm. Sci.* **2002**, *91*, 1308.
37. Wilson, C.C. *Z. Kristallogr.* **2000**, *215*, 693.
38. Burgina, E.B.; Baltakhinov, V.P.; Boldyreva, E.V.; Shakhtshneider, T.P. *Russ. Zhurn. Strukt. Khim. (Russ J. Struct. Chem.)* **2004**, *45*, 70.
39. Binev, I.G.; Vassileva-Boyadjieva, P.; Binev, Y.I. *J. Mol. Struct.* **1998**, *447*, 235.
40. Marsh, R.E.; *Acta Crystallogr.* **1958**, *11*, 654.
41. Iitaka, Y. *Nature*, **1959**, *4658*, 390.
42. Iitaka, Y. *Acta Crystallogr.* **1960**, *13*, 35.
43. Iitaka, Y. *Acta Crystallogr.* **1961**, *14*, 1.
44. Boldyreva, E.V.; Drebuschak, T.N.; Shutova, E.S. *Z. Kristallogr.* **2003**, *218*, 366.
45. Dunitz, J.; Bernstein, A. *Acc. Chem. Res.* **1995**, *28*, 193.
46. Boldyreva, E.V.; Drebuschak, V.A.; Drebuschak, T.N.; Paukov, I.E.; Kovalevskaya, Yu.A., Shutova, E.S. *J. Therm. Analys. Calorim.* **2003**, *73*, 409.
47. Boldyreva, E.V.; Drebuschak, V.A.; Drebuschak, T.N.; Paukov, I.E.; Kovalevskaya, Yu.A.; Shutova, E.S. *J. Therm. Analys. Calorim.* **2003**, *73*, 419.
48. Sakai, H.; Hosogai, H.; Kawakita, T.; Onuma, K.; Tsukamoto, K. *J. Cryst. Growth* **1992**, *116*, 421.
49. Perlovich, G. L.; Hansen, L. K.; Bauer-Brandl A. *J. Therm. Analys. Calorim.* **2001**, *66*, 699.
50. Weissbuch, I.; Lahav, M.; Leiserowitz, L. *Cryst. Growth Design* **2003**, *3*, 125.
51. Zaccaro, J.; Matic, J.; Myerson, A. S.; Garetz, B. A. *Cryst. Growth Design* **2001**, *1*, 5.
52. Garetz, B. A.; Matic, J.; Myerson, A. S. *Phys. Rev. Lett.* **2002**, *89*, 175501.
53. Weissbuch, I.; Addadi, L.; Berkovitch-Yellin, Z.; Gati, E.; Weinstein, S.; Lahav, M.; Leiserowitz, L. *J. Amer. Chem. Soc.* **1983**, *105*, 6613.
54. Weissbuch, I.; Addadi, L.; Berkovitch-Yellin, Z.; Gati, E.; Lahav, M.; Leiserowitz, L. *Nature* **1984**, *310*, 161.
55. Shimon, L.J.W.; Wireko, F.C.; Wolf J. et. al. *Mol. Cryst. Liq. Cryst.* **1986**, *137 (1-4)*, 67.
56. Shimon, L. J. W.; Lahav, M.; Leiserowitz, L.; *Nouv. J. Chim.* **1986**, *10*, 723.
57. Weissbuch, I.; Leiserowitz, L.; Lahav, M. *Adv. Mater.* **1994**, *6*, 953.

58. Weissbuch, I.; Popovitz-Biro, R.; Lahav, M.; Leiserowitz, L. *Acta Cryst.* **1995**, *B51*, 115.
59. Landau, E.M.; Levanon, M.; Leiserowitz, L.; Lahav, M.; Sagiv, J. *Nature* **1985**, *318* (6044), 353.
60. Gavezzotti, A. *Crystallogr. Rev.* **1998**, *7*, 5.
61. Leonidov, N.B.; *Mendeleev Chem. J.* **2000**, *41*, 7.
62. Carter, P.W.; Hillier, A.C.; Ward, M.D. *J. Amer. Chem. Soc.* **1994**, *116*, 944.
63. Gidalevitz, D.; Feidenhans'l, R.; Matlis, S.; Smilgies, D.-M.; Christensen, M.J.; Leiserowitz, L. *Angew. Chem. Int. Ed. Engl.* **1997**, *36*, 955.
64. Gidalevitz, D.; Feidenhans'l, R.; Smilgies, D.-M.; Leiserowitz, L. *Surface Rev. and Letters* **1997**, *4*, 721.
65. Mccrone, W. C. In: *Physics and Chemistry of the Organic Solid State*; Vol. 2, Fox, D.; Labes, M. M.; Weissberger, A. Eds.; Interscience: New York, 1965; pp 726-767.
66. Bernstein, J. *Polymorphism in Molecular Crystals*; IUCr Monographs on Crystallography 14, Oxford Science Publications, Clarendon Press: Oxford, 2002.
67. Goryainov, S.V.; Kolesnik, E.N.; Boldyreva, E.V. *Physica C*, submitted.
68. Drebuschak, T.N.; Kolesnik, E.N.; Boldyreva, E.V.; *Russ. J. of Struct. Chem.* **2004**, accepted.
69. Boldyreva, E.V.; Ahsbahs H.; Weber H.-P. *Z. Kristallogr.* **2003**, *218*, 231.
70. Murli, C.; Sharma, S.M.; Karmakar, S.; Sikka, S. K. *Physica B* **2003**, *339*, 23.
71. Goryainov, S.V.; Kolesnik, E.N.; Boldyreva, E.V. *Proceed. III Intern. Confer. High-Pressure Physics* (Chernogolovka, 1-3 June 2004), P-27.
72. Goryainov, S.V.; Kolesnik, E.N.; Boldyreva, E.V. *Physica C* **2004**, submitted.
73. Boldyreva, E.V.; Ivashetskaya, S.N.; Sowa, H.; Ahsbahs, H.; Weber, H.-P. *Doklady Phys. Chem.* **2004**, *396*, 358.
74. Boldyreva, E.V.; Ivashetskaya, S.N.; Sowa, H.; Ahsbahs, H.; Weber, H.-P. *Z. Kristallogr.* **2004**, accepted.
75. Benedetti, E.; Pedone, C.; Sirigu, A. *Gazzetta Chim. Italiana* **1973**, *103*, 555.
76. Kistenmacher, T. J.; Rand, G. A.; Marsh R. E. *Acta Crystallogr.* **1974**, *B30*, 2573.
77. Boldyreva, E.V.; Kolesnik, E. N.; Drebuschak, T.N.; Ahsbahs, H.; Beukes, J. A.; Weber, H.-P., *Z. Krist.* **2004**, accepted.
78. Boldyreva, E.V.; Kivikoski J.; Howard, J.A.K., *Acta Crystallogr.* **1997**, *B53*, 394.
79. Boldyreva, E.V.; Kivikoski, J.; Howard, J.A.K. *Acta Crystallogr.* **1997**, *B53*, 405.
80. Boldyreva, E.V.; Ahsbahs, H.; Naumov, D.Yu. *Acta Crystallogr.* **1998**, *B54*, 798.
81. Boldyreva, E.V.; Shakhshneider, T. P.; Ahsbahs H., Sowa H., Uchtmann H., *J. Struct. Chem.* **2002**, *43*, 107.
82. Katrusiak, A. *Acta Crystallogr.* **1990**, *B46*, 246.
83. Katrusiak, A. *Acta Crystallogr.* **1991**, *B47*, 398.
84. Goryainov, S.V.; Kolesnik, E.N.; Boldyreva, E.V. *Doklady Phys. Chem.* **2004**, submitted.
85. Boldyreva, E.V.; Drebuschak, T.N.; Kolesnik, E.N.; Sowa, H.; Ahsbahs, H.Z. *Kristallogr.* **2004**, submitted.